PHILOSOPHICAL TRANSACTIONS A

rsta.royalsocietypublishing.org

Research

Cite this article: Cordero P, Risso D, Soto R. 2015 Effect of the vibration profile on shallow granular systems. *Phil. Trans. R. Soc. A* **373**: 20150116.
http://dx.doi.org/10.1098/rsta.2015.0116

Accepted: 29 July 2015

One contribution of 13 to a theme issue 'Topics on non-equilibrium statistical mechanics and nonlinear physics (II)'.

Subject Areas:
statistical physics

Keywords:
granular systems, phase separation, low-dimensional dynamical systems, numerical simulations

Author for correspondence:
Patricio Cordero
e-mail: pcordero@dfi.uchile.cl

Effect of the vibration profile on shallow granular systems

Patricio Cordero[1], Dino Risso[2] and Rodrigo Soto[1]

[1]Departamento de Física, Facultad de Ciencias, Físicas y Matemáticas, Universidad de Chile, Santiago, Chile
[2]Departamento de Física, Facultad de Ciencias, Universidad del Bio-Bio, Concepcion, Chile

We describe the collective behaviour of a system of many inelastic spherical particles inside a box which is being periodically vibrated. The box is shallow, with large horizontal dimensions, while the height is less than two particle diameters. The vibrations are not symmetric: the time the box is moving up is, in general, different from the time it is moving down. The limit cycles of isolated grains are largely affected by the asymmetry of the vibration mode, increasing the size in phase space of the chaotic regions. When many grains are placed in the box, the phase separation between dense, solid-like regions, coexisting with fluid-like regions takes place at smaller global densities for asymmetric vibration profiles. Besides, the order parameter of the transition takes larger values when asymmetric forcing is used.

1. Introduction

Granular systems, characterized by the dissipative collisional dynamics of macroscopic objects, still defy our understanding. When energy is injected at a high enough rate to compensate for the dissipated energy, dynamical states are generated. Granular media, in many aspects, resemble molecular fluids. However, the energy dissipated at every collision permanently keeps those systems in a non-equilibrium state. The origin of the non-equilibrium states is that energy injected by one mechanism—for example, collisions with the walls—is dissipated by a different one, interparticle collisions. A necessary condition for equilibrium would be detailed balance which is not present in our system.

It has been shown that varying the injection mechanism generates non-equilibrium states with different properties. For example, the shear viscosity varies from case to case. Compare the outcomes in [1–4],

THE ROYAL SOCIETY PUBLISHING

where the inelastic hard sphere model is used in all cases, but the driving mechanism is different. Hence, it is interesting to study the different behaviours of the system when different energy injection mechanisms are used.

A particular geometry to study granular systems that has gained interest is the quasi-two-dimensional (Q2D) configuration. In this case, grains are put in a shallow box: large horizontal dimensions and a rather small vertical one. The box is vertically vibrated and the spherical grains gain energy colliding with the top and bottom plates. This energy is partly transferred to the horizontal directions through collisions.

Using shallow boxes has many advantages. In experiments, it allows the dynamics of the granular layer to be fully visualized by imaging the system, as all particles can be seen and recorded with a camera from the top. This makes it possible to accurately study the system in a microscopic way, as particle positions and velocities can be measured for most particles at any time. Also the collective behaviour can be captured [5–10]. Implied by the energy injection mechanism, the horizontal kinetic energy of the grains can be quite different from the vertical kinetic energy [11,12].

When the height of the box is less than twice the particle diameter, we have a particular and relevant case: no two particles can be on top of one another. Here, gravity does not play a direct role in the horizontal dynamics and the indirect effects can be controlled and reduced by means of increasing the dimensionless acceleration of the box. More importantly, gravity is perpendicular to the eventual directions of phase separation, allowing one to discard many known mechanisms. Nevertheless, experiments and simulations have shown that segregation can also take place between grains that differ in size or mass [12,13].

It has been observed that a particular phase separation takes place in shallow boxes: grains form solid-like regions surrounded by fluid-like ones having high contrasts in density, local order and granular temperature [5,6]. This phase separation is driven by the negative compressibility of the effective two-dimensional fluid [7] and, depending on the height of the box, it can be either of first or second order [14,15].

In the present article, we study the role that the energy injection plays in the phase separation in Q2D systems. To do so, keeping the material properties and geometry of the system unchanged, we vary the waveform profile of the vibration. That is, we change the pure sinusoidal profile, where the upward and downward phases are symmetric, to asymmetric profiles where both phases take different times. Under these conditions, we first analyse the dynamics of isolated grains looking for the limit cycles that each one of them develops. For the case of an isolated particle with no top wall, see [16–19]. Next, we consider dense regimes where the grains interact so that phase separation may take place. It is found that asymmetric vibration profiles increase the size of the chaotic regions in phase space and also facilitate phase separation. Our main tools are event-driven molecular dynamics simulations, making use of our own quite efficient strategy [20–25] (see also [26]).

2. The model

(a) System set-up

The grains are inelastic hard spheres with rotational degrees of freedom. These particles are in a vertically vibrated *shallow box*: namely we consider granular systems in a box with a height of the order of two particle diameters and much larger horizontal dimensions. Collisions are characterized by normal and tangential restitution coefficients as well as friction coefficients.

The diameter σ of the particles, the acceleration of gravity g and the mass m of the particles are used to define the dimensionless expressions in this article, except that time is measured in oscillation periods, $T = 2\pi/\omega$. The horizontal lengths of the box L_x and L_y will be different in different simulations, although in all cases they will be large compared with the

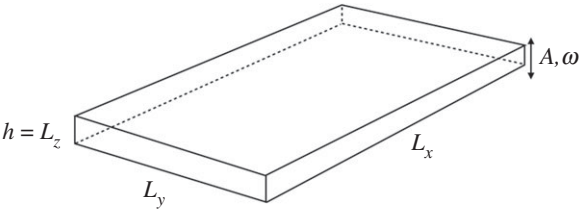

Figure 1. Configuration of the Q2D granular system. The box is periodic in the horizontal directions, while it is confined by the top and bottom hard walls. The inner height is h. Grains are placed inside the box, which is vertically vibrated with amplitude A and angular frequency ω.

confinement height $h = L_z$, which is taken to be between 1.8σ and 1.82σ. Simulations to study the phase separations are done with $L_z \ll L_y \ll L_x$, where the system remains homogeneous in the y-direction, allowing us to measure the density contrast between the solid-like cluster and the surrounding liquid-like phase. The vibration is characterized by the amplitude A and frequency ω (figure 1). Finally, collisions are characterized by the following mechanical parameters: normal and tangential restitution coefficients r_n and r_t, while the static and dynamic friction coefficients are μ_s and μ_d. Their specific values will be given in each case.

(b) Symmetric profiles: sinusoidal versus parabolic

It may seem natural to consider sinusoidal vibrations, but we have studied systems for which the vibration cycle is characterized by four separate parabolic movements in the sense that the height depends quadratically in time. The acceleration is piecewise constant, with values $a = \pm 8A\omega^2/\pi^2$. This parabolic movement is described in detail in the next subsection. It will be interesting to observe that for a given vibration frequency, there is a range of amplitudes for which the system behaves almost as if there were sinusoidal vibrations.

(c) Asymmetric profiles

In our studies, energy is injected to the system by means of vertically vibrating the box using asymmetric modes where, again, the acceleration is piecewise constant. We define the *asymmetry coefficient* β $(0 < \beta < 1)$, which divides the period in two intervals of size βT and $(1-\beta)T$. In the first interval, the box moves down with accelerations $a = \pm 2A\omega^2/\beta^2\pi^2$, while in the second one the box moves up with accelerations $a = \pm 2A\omega^2/(1-\beta)^2\pi^2$.

The heights Z of the top $(+)$ and bottom $(-)$ walls of the box are given by

$$Z_\pm(t;\beta) = \pm\frac{h}{2} + \alpha(\tau;\beta)A, \tag{2.1}$$

where $\tau = t \mod T$ and

$$\alpha(\tau;\beta) = \begin{cases} \dfrac{1}{\beta^2T^2}(\beta^2T^2 - 4\tau^2) & 0 \le \tau \le \dfrac{\beta T}{2} \\ \dfrac{1}{\beta^2T^2}(2\tau - \beta T)(2\tau - 3\beta T) & \dfrac{\beta T}{2} \le \tau \le \beta T \\ \dfrac{1}{(1-\beta)^2T^2}(2\tau + (1-3\beta)T)(2\tau - (1+\beta)T) & \beta T \le \tau \le \dfrac{(1+\beta)T}{2} \\ \dfrac{1}{(1-\beta)^2T^2}(2\tau - (3-\beta)T)((1+\beta)T - 2\tau) & \dfrac{(1+\beta)T}{2} \le \tau \le T. \end{cases} \tag{2.2}$$

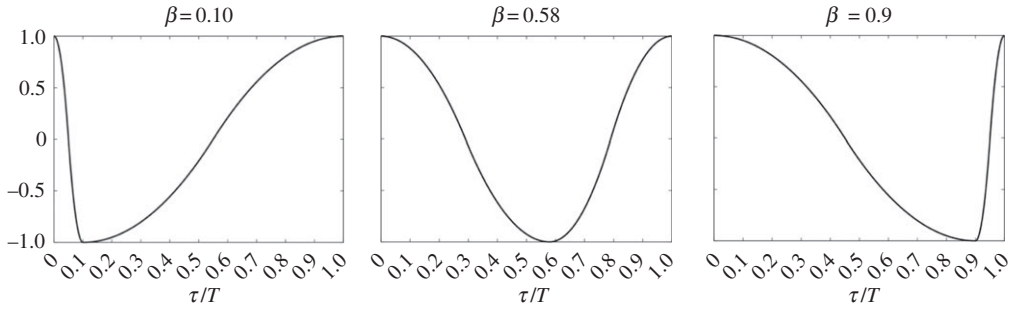

Figure 2. The function $\alpha(\tau;\beta)$ that defines the box-oscillation profile for different values of the asymmetry parameter β. For $\beta < 1/2$, the downwards interval takes a shorter time than the upward movement (left) and conversely for $\beta > 1/2$ (right). For $\beta = 1/2$, the function $\alpha(\tau;\beta)$ resembles $\cos(2\pi\tau/T)$.

This function is continuous and has continuous first derivatives. The first derivative of $\alpha(\tau;\beta)$ vanishes at $\tau = 0$, at $\tau = \beta T$ and at $\tau = T$. For $\beta = 1/2$, this quadratic function roughly resembles $\cos(2\pi\tau/T)$ (figure 2).

The control parameters are the asymmetry parameter β, the amplitude A and angular frequency $\omega = 2\pi/T$ of the oscillations. The latter is characterized by the dimensionless acceleration $\Gamma = A\omega^2/g$ and dimensionless velocity $\zeta = A\omega/\sqrt{g\sigma}$.

3. A single particle in the vibrating box

In the case of shallow boxes, it is important to understand first the movement of a single particle. There are conditions under which the particle ends up in permanent contact with the base of the box. But if $A\omega^2/g$ is larger than unity, such a situation cannot occur. Next, it may happen that the energy injected to the particle by the base is not enough for the particle to reach the upper wall in the long-term evolution. We consider conditions under which neither of these last two cases can take place.

If the single particle is left bouncing for a sufficiently large time, its angular and horizontal translation velocities vanish so that the movement of the particle becomes strictly one-dimensional and the friction coefficients as well as the tangential restitution coefficient become irrelevant. There is a wide range of amplitudes and frequencies for which the particle reaches this quite simple limit cycle characterized by two velocities: the velocities with which the particle bounces off the two horizontal walls.

Increasing the vibration frequency or the amplitude, the limit cycle of the single particle reaches a threshold above which the limit cycle suffers a bifurcation. Now the grain bounces twice at the top and bottom walls before repeating its movement. Hence, the new limit cycle takes twice the time associated to the limit cycle just before the bifurcation. There is a chain of bifurcations of this type until the bouncing of the single particle becomes chaotic. Some cases of the resulting limit cycles are presented in figure 3. All this can be appreciated in figure 4 where it is seen that other modes appear as the amplitude grows, that is, the particle has more than one bouncing mode for a given value of the amplitude. Figure 4 includes in red the bouncing velocities when the vibration is sinusoidal with the same frequency and amplitude as our parabolic vibration. To our surprise, when $\beta = 0.5$, the bouncing velocities are almost exactly the same until about $A/\sigma = 0.2$.

Figure 5 presents a qualitative picture of the possible outcomes. Different colours are used to represent the single period, double period and chaotic motion cases. The comparison shows how similar is the behaviour with sinusoidal and parabolic profiles, except that for large amplitudes the parabolic profiles are more regular. In both cases, a band of chaotic motion is present for small amplitudes.

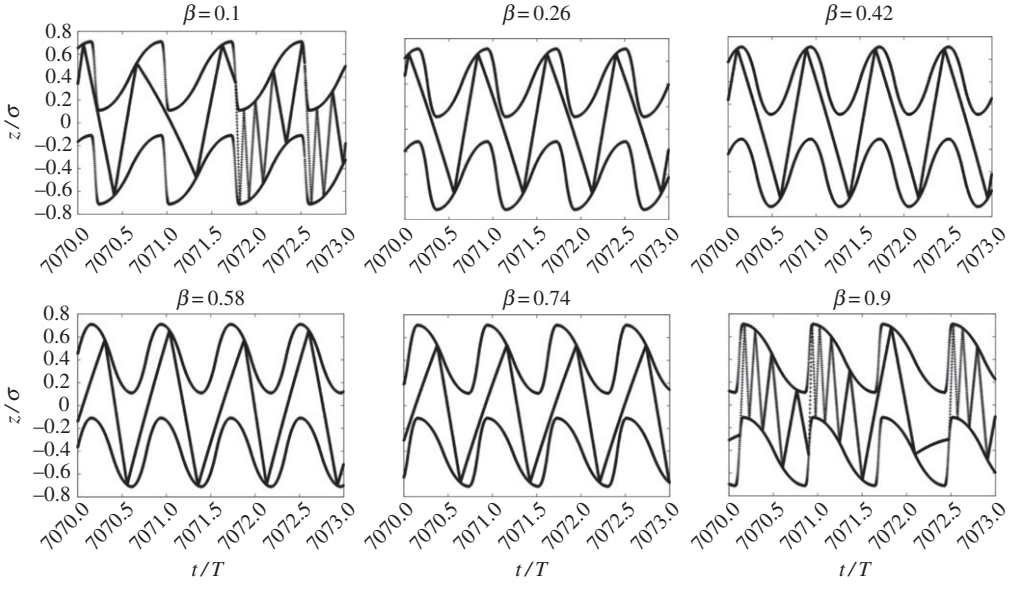

Figure 3. A single particle in the shallow box subject to vibrations having the same Γ and ζ but different values of β may have quite different stationary bouncing modes. In this example, we chose $\Gamma = 18.56$ and $\zeta = 2.32$.

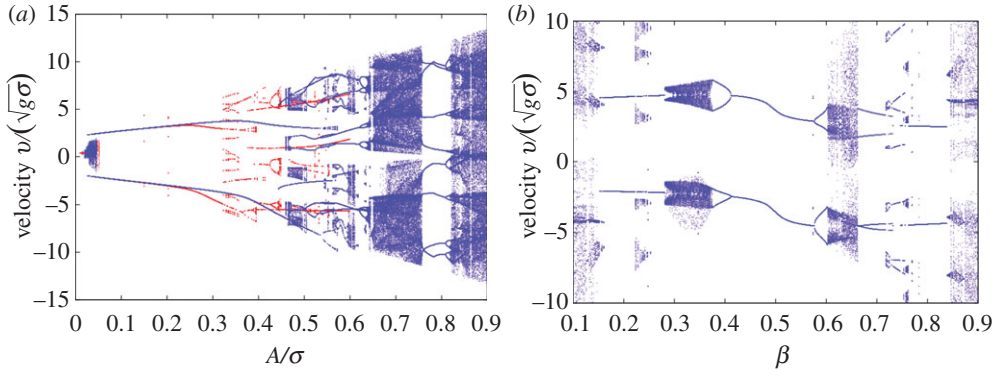

Figure 4. Bouncing velocities after colliding with the top and bottom walls of the shallow box once the particle has reached a steady state. (*a*) Varying the vibration amplitude A in the case of the sinusoidal (red, light grey) and bi-parabolic (blue, dark grey) symmetric profiles ($\beta = 1/2$). (*b*) Varying the asymmetry parameter β with fixed vibrating amplitude $A/\sigma = 0.3$. The asymmetry on the obtained velocities around $\beta = 1/2$ is due to the presence of gravity. In both figures, $\omega = 8\sqrt{g/\sigma}$, $r_n = 0.8$ and $h = 1.82\sigma$. In (*b*), $\Gamma = 19.2$ and $\zeta = 2.4$. (Online version in colour.)

Using the same analysis, we consider the asymmetric profile, varying the parameter β in the case where in the symmetric profile the limit cycle consists of a single bounce on the top and bottom walls. Figure 2 shows that close to the symmetric case ($\beta \approx 0.5$), the limit cycle is perturbed, keeping its qualitative behaviour but changing the values of the bouncing velocities. Further away from the symmetric condition, period doubling and chaos appear. The qualitative plots in figure 6 confirm this result. The most regular motion is obtained in the vicinity of $\beta = 0.5$. For intermediate values of β, figure 6 shows that the effect of gravity is obvious in the case of smaller values of ζ, while for ζ large (small g) the structure of the figure is weakly dependent on ζ.

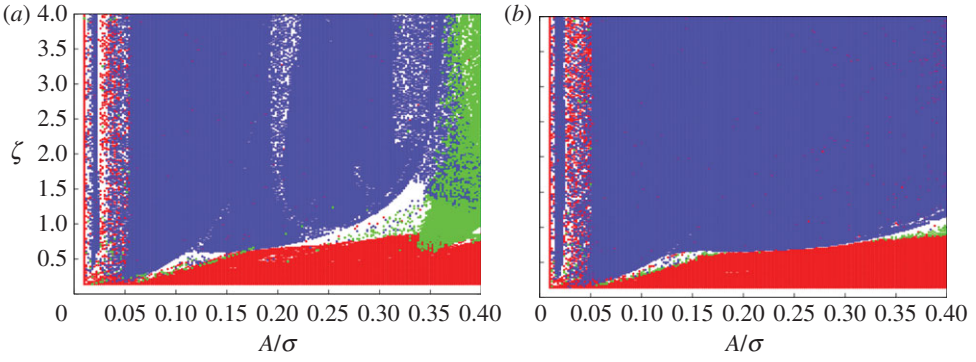

Figure 5. Map in the A–ζ plane of the qualitative characterization of the limit cycles for the sinusoidal profile (*a*) and for the symmetric $\beta = 1/2$ parabolic profile (*b*). The possible outcomes are: bouncing only with the bottom wall with period T (red, grey), bouncing with the top and bottom walls with period T (blue, dark grey), bouncing with the bottom and top walls with double period $2T$ (green, light grey) and more complex states (white). In both cases, $h = 1.8\sigma$ and $r_n = 0.8$. (Online version in colour.)

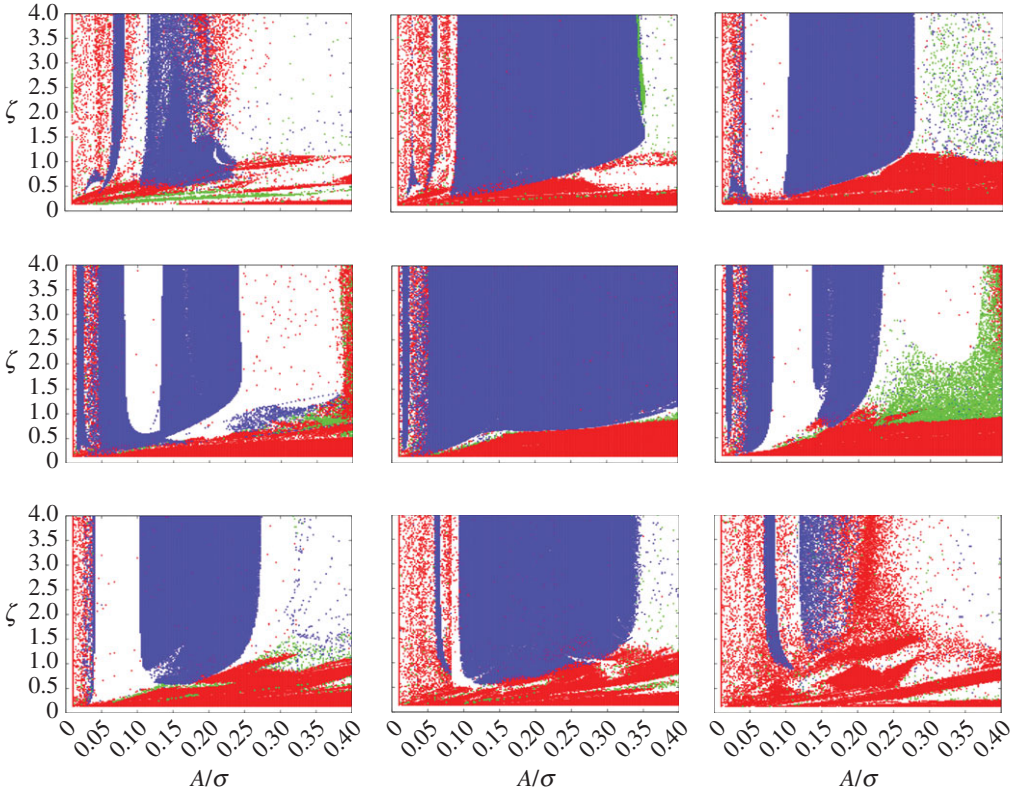

Figure 6. Map in the A–ζ plane of the qualitative characterization of the limit cycles for different values of β using the same colour coding as in figure 5. From left to right, top: $\beta = 0.1, 0.2, 0.3$, middle: $\beta = 0.4, 0.5, 0.6$, bottom: $\beta = 0.7, 0.8, 0.9$. In all cases, $h = 1.8\sigma$ and $r_n = 0.8$. (Online version in colour.)

4. Phase separation

In the case of systems composed by a single species of granular matter, there are conditions under which the system separates into high- and low-density zones [7]. The results of the previous section illustrate a central point: the form of the vibration—determined by the parameter β—has

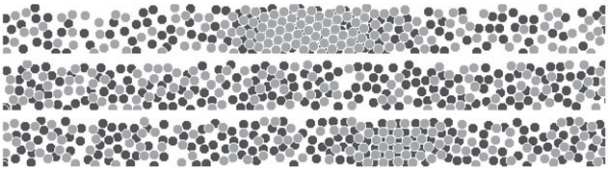

Figure 7. Top view of a shallow system in a rather narrow box ($L_y \ll L_x$) in a typical state for a system with common values for all the parameters except for the value of β. Particles are all the same, but they are represented by black circles if their height is below half the height of the box, otherwise they are represented by grey circles. From top down, $\beta = 0.1$, $\beta = 0.5$ and $\beta = 0.75$. The first and third cases have notoriously stable phase separated states, showing large density contrasts. In all cases, $N = 410$, $L_x = 90.01\sigma$, $L_y = 4.65\sigma$, $h = 1.8\sigma$, $r_n = r_t = 0.91$, $\mu_d = 0.10$, $\mu_s = 0.17$, $\omega = 10\sqrt{g/\sigma}$ and $A = 0.29\sigma$ implying $\zeta = 2.9$ and $\Gamma = 29.0$.

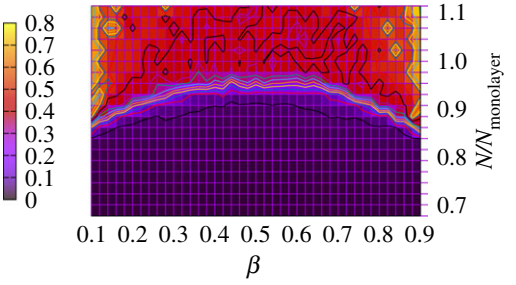

Figure 8. Density contrast c in the β–$N/N_{\text{monolayer}}$ plane for a system with $L_z = 1.8\sigma$ and $L_x \times L_y = 90\sigma \times 4.65\sigma$ and vibration parameters $\tilde{\omega} = \omega/\sqrt{g/\sigma} = 3$ and $A = 0.29\sigma$; $\zeta = 0.87$, $\Gamma = 2.61$. The inelasticity and friction grain–grain and grain–wall coefficients are $r_n = r_t = 0.91$ and $\mu_d = 0.10$, $\mu_s = 0.17$. (Online version in colour.)

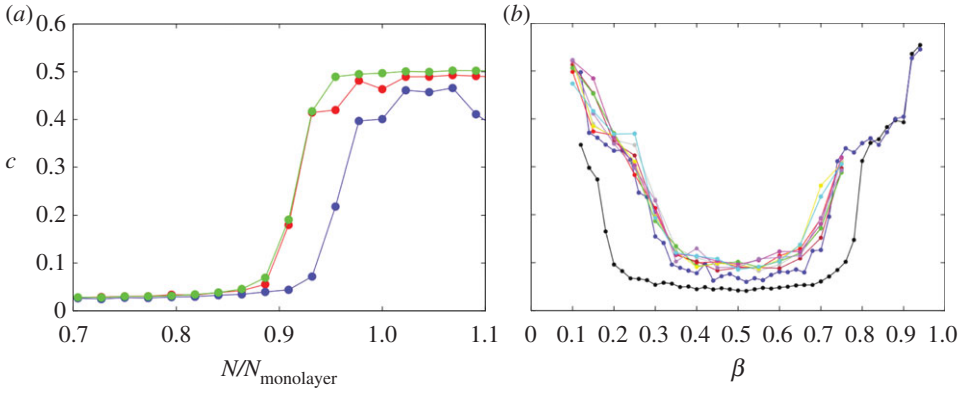

Figure 9. (*a*) Density contrast against $N/N_{\text{monolayer}}$ for $\beta = 0.22$ (red), $\beta = 0.5$ (blue) and $\beta = 0.78$ (green). The amplitude is fixed to $A = 0.29\sigma$, while the dimensionless frequency takes the value $\tilde{\omega} = \omega/\sqrt{g/\sigma} = 3$. (*b*) Density contrast against β for a system with $N = 410$ grains ($N/N_{\text{monolayer}} = 0.93$). The amplitude is fixed to $A = 0.29\sigma$, while the dimensionless frequency takes the values $\tilde{\omega} = 2$ (black), $\tilde{\omega} = 3$ (blue), $\tilde{\omega} = 5$ (grey), $\tilde{\omega} = 10$ (red), $\tilde{\omega} = 15$ (brown), $\tilde{\omega} = 20$ (green), $\tilde{\omega} = 25$ (yellow), $\tilde{\omega} = 30$ (magenta), $\tilde{\omega} = 35$ (purple) and $\tilde{\omega} = 40$ (cyan). In all cases, $L_z = 1.8\sigma$, $L_x \times L_y = 90\sigma \times 4.65\sigma$ and the inelasticity and friction grain–grain and grain–wall coefficients are $r_n = r_t = 0.91$ and $\mu_d = 0.10$, $\mu_s = 0.17$. (Online version in colour.)

an important effect on the way the system behaves. This is illustrated in figure 7 which shows a characteristic state of a vibrated granular system in a narrow three-dimensional box: depending on the value of β, the system may or may not present phase separation. Indeed, with all other

parameters fixed to a case where the symmetric case would yield a state with no phase separation, forcing with asymmetric profiles induces phase separation.

For a quantitative analysis, we define the *contrast* observable c, which is the ratio between the smaller and larger observed area densities: $c = (n_{\max} - n_{\min})/(n_{\max} + n_{\min})$. In the case of the system shown in figure 7, which is strictly three dimensional, the density is evaluated considering many transversal strips and calculating the area density in each strip, defined using the projection of the particles in each two-dimensional strip.

Figure 8 shows that, in agreement with the snapshots in figure 7, the density contrast is larger when β is away from the symmetric case $\beta = 0.5$. A transition line can be identified where there is a steep increase in c. This transition line indicates that away from the symmetric case, a smaller number of particles is needed to produce the phase separation. This is clearly presented in figure 9*a*, where the contrast is shown as a function of the number of particles for three values of β. A clear transition is observed, with a critical number of particles that is larger for $\beta = 1/2$.

Figure 9*b* presents the contrast c as a function of β for a fixed number of particles and different values of ω. The collapse between the majority of the curves shows that the major impact in the phase separation is the shape of the vibration rather than the energy injection rate.

5. Conclusion

In this article, we have studied the effect of changing the energy injection profile of a box of vibrofluidized shallow granular media, where the box moves vertically in a periodic way. With this aim, we modify the oscillation profile. Originally, the profile was symmetric with piecewise constant accelerations, mimicking a sinusoidal oscillation. This profile was changed to an asymmetric one, still with piecewise constant accelerations, where the downward and upward phases take different fractions of the oscillation period: β and $1 - \beta$, respectively.

Single isolated grains reach states where the motion is purely vertical. These states can be periodic in the form of limit cycles with the same period as the box or with a period that is an integer multiple of the box period. Also chaotic or irregular motion is possible. The effect of moving towards asymmetric forcing is to increase the region in parameter space where chaotic motion is observed. Conversely, it is more probable to find regular motion with the same period as the box for the symmetric forcing.

The asymmetric forcing also has an effect on the phase separation between dense and dilute regions when many particles are placed in the box. The phase separation takes place for smaller number of particles when the forcing is asymmetric. The previous result suggests that other ways of increasing the asymmetry could also be efficient in producing phase separation. As an extreme case, we consider a sawtooth profile at high frequency and small amplitude, such that particles always meet the walls at the same position and approaching the particles with a fixed velocity. Figure 10 shows that indeed phase separation takes place and high contrast states can be attained.

It remains as an open question if there is a relation between the accessibility to chaotic behaviour for single particles far from the symmetric profile and the enhanced phase separation in the collective dynamics with many particles.

In [7], it was shown that the origin of the phase separation is a negative compressibility region in the effective equation of state of the pressure as a function of density $p = p(n)$. This equation of state emerges as a consequence of the temperature being governed by the density under high vertical confinement, with $T(n)$ a monotonically decreasing function. Then, equations of state $p = p(n, T)$ derived from kinetic theory, with positive compressibility can turn into effective equations of state with negative compressibility and van der Waals loops [27]. An attempt to understand why it is that for β far from 0.5 a phase separation takes place for lower densities, it would be necessary to study in the stationary regime the enslaving $T(n)$, which will depend on β. This analysis needs the study of the limit cycles coupled with the three-dimensional collisions that transfer energy from the vertical to the horizontal degrees of freedom. This analysis, beyond the scope of this article, is postponed for a future study.

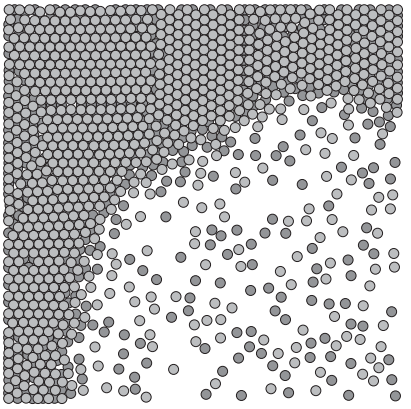

Figure 10. Top view of a shallow system in a box of square basis. This is a typical state once phase separation has taken place. The black/grey colouring is as in figure 7. The limit of infinitely rapid vibration is taken ($A \to 0$, $\omega \to \infty$, while $A\omega = V_0 =$ constant) for a sawtooth profile with no gravity. This state was obtained using $N = 1732$, $L_x = L_y = 40\sigma$, $L_z = 1.9\sigma$, $r_n = r_t = 0.7$ (grain–grain), $r_n = r_t = 0.999$ (wall–grain) and $\mu_s = \mu_d = 0.1$.

The results of the present article as well as others confirm that the properties of non-equilibrium systems depend not only on the internal dynamics but also on the energy injection mechanism. Consistent with this, it should be said that there is no guarantee that the conclusion drawn here could be valid for other forcing mechanisms.

Authors' contributions. P.C. and D.R. carried out the simulations. All authors participated in the design of the simulations, analysis of the results and writing of the manuscript.

Competing interests. We declare we have no competing interests.

Funding. This research was supported by Fondecyt grant nos. 1120775 and 1140778.

References

1. Brey JJ, Dufty JW, Kim CS, Santos A. 1998 Hydrodynamics for granular flow at low density. *Phys. Rev. E* **58**, 4638–4653. (doi:10.1103/PhysRevE.58.4638)
2. Santos A, Garzó V, Dufty JW. 2004 Inherent rheology of a granular fluid in uniform shear flow. *Phys. Rev. E* **69**, 061303. (doi:10.1103/PhysRevE.69.061303)
3. Cordero P, Risso D, Soto R. 2005 Steady quasi-homogeneous granular gas state. *Phys. A* **356**, 54–60. (doi:10.1016/j.physa.2005.05.012)
4. Soto R, Risso D, Brito R. 2014 Shear viscosity of a model for confined granular media. *Phys. Rev. E* **90**, 062204. (doi:10.1103/PhysRevE.90.062204)
5. Olafsen JS, Urbach JS. 1998 Clustering, order, and collapse in a driven granular monolayer. *Phys. Rev. Lett.* **81**, 4369–4372. (doi:10.1103/PhysRevLett.81.4369)
6. Prevost A, Melby P, Egolf DA, Urbach JS. 2004 Non-equilibrium two-phase coexistence in a confined granular layer. *Phys. Rev. E* **70**, 050301. (doi:10.1103/PhysRevE.70.050301)
7. Clerc MG, Cordero P, Dunstan J, Huff K, Mujica N, Risso D, Varas G. 2008 Liquid–solid-like transition in quasi-one-dimensional driven granular media. *Nat. Phys.* **4**, 249–254. (doi:10.1038/nphys884)
8. Schnautz T, Brito R, Kruelle CA, Rehberg I. 2005 A horizontal Brazil-nut effect and its reverse. *Phys. Rev. Lett.* **95**, 028001. (doi:10.1103/PhysRevLett.95.028001)
9. Chung FF, Liaw SS, Ju CY. 2009 Brazil nut effect in a rectangular plate under horizontal vibration. *Gran. Matter* **11**, 79–86. (doi:10.1007/s10035-008-0122-2)
10. Pacheco-Vazquez F, Caballero-Robledo GA, Ruiz-Suarez JC. 2009 Superheating in granular matter. *Phys. Rev. Lett.* **102**, 170601. (doi:10.1103/PhysRevLett.102.170601)
11. Melby P, Reyes FV, Prevost A, Robertson R, Kumar P, Egolf DA, Urbach JS. 2005 The dynamics of thin vibrated granular layers. *J. Phys. Condens. Matter* **17**, S2689–S2704. (doi:10.1088/0953-8984/17/24/020)

12. Rivas N, Cordero P, Risso D, Soto R. 2011 Segregation in quasi-two-dimensional granular systems. *New J. Phys.* **13**, 055018. (doi:10.1088/1367-2630/13/5/055018)
13. Rivas N, Ponce S, Gallet B, Risso D, Soto R, Cordero P, Mujica N. 2011 Sudden chain energy transfer events in vibrated granular media. *Phys. Rev. Lett.* **106**, 088001. (doi:10.1103/PhysRevLett.106.088001)
14. Castillo G, Mujica N, Soto R. 2012 Fluctuations and criticality of a granular solid–liquid-like phase transition. *Phys. Rev. Lett.* **109**, 095701. (doi:10.1103/PhysRevLett.109.095701)
15. Castillo G, Mujica N, Soto R. 2015 Universality and criticality of a second-order granular solid–liquid-like phase transition. *Phys. Rev. E* **91**, 012141. (doi:10.1103/PhysRevE.91.012141)
16. Mehta A, Luck JM. 1990 Novel temporal behavior of a nonlinear dynamical system: the completely inelastic bouncing ball. *Phys. Rev. Lett.* **65**, 393–396. (doi:10.1103/PhysRevLett.65.393)
17. Mehta A, Luck JM. 1993 Bouncing ball with a finite restitution: chattering, locking, and chaos. *Phys. Rev. E* **48**, 3988–3997. (doi:10.1103/PhysRevE.48.3988)
18. Szymanski K, Labaye Y. 1999 Energy dissipation in the dynamics of a bouncing ball. *Phys. Rev. E* **59**, 2863–2871. (doi:10.1103/PhysRevE.59.2863)
19. Barroso JJ, Carneiro MV, Macau EEN. 2009 Bouncing ball problem: stability of the periodic modes. *Phys. Rev. E* **79**, 026206. (doi:10.1103/PhysRevE.79.026206)
20. Marin M, Risso D, Cordero P. 1993 Efficient algorithms for many-body hard particle molecular dynamics. *J. Comput. Phys.* **109**, 306–317. (doi:10.1006/jcph.1993.1219)
21. Cordero P, Risso D, Marin M. 1995 Efficient simulations of microscopic fluids: algorithm and experiments. *Chaos Solitons Fractals* **6**, 95–104. (doi:10.1016/0960-0779(95)80016-A)
22. Marin M, Cordero P. 1995 An object oriented C++ approach for discrete event simulation of complex and large systems of many moving objects. In *Proc. 28th Annual Simulation Symp., Phoenix, AZ, USA, 9–13 April 1995* (eds G Chiola, A Ferscha, E Kortright), pp. 288–295. (doi:10.1109/SIMSYM.1995.393570)
23. Marín M, Cordero P. 1995 An empirical assessment of priority queues in event-driven molecular dynamics simulation. *Comput. Phys. Commun.* **92**, 214–224. (doi:10.1016/0010-4655(95)00120-2)
24. Marin M, Cordero P. 1996 Hashing-cell combination for boundless space event-driven molecular dynamics. In *8th Joint EPS-APS Int. Conf. on Physics Computing, Krakow, Poland, September 1996* (eds P Borcherds, M Bubak), pp. 315–318. Singapore: World Scientific.
25. Cordero P, Risso D. 1997 Microscopic computer simulation of fluids. In *Fourth Granada lectures in computational physics* (eds PL Garrido, J Marro). Lecture Notes in Physics, vol. 493, pp. 83–134. Berlin, Germany: Springer. (doi:10.1007/BFb0105986)
26. González S, Risso D, Soto R. 2009 Extended event driven molecular dynamics for simulating dense granular matter. *Eur. Phys. J. Spec. Top.* **179**, 33–41. (doi:10.1140/epjst/e2010-01192-4)
27. Cartes C, Clerc MG, Soto R. 2004 van der Waals normal form for a one-dimensional hydrodynamic model. *Phys. Rev. E* **70**, 031302. (doi:10.1103/PhysRevE.70.031302)